Surface & Coatings Technology 204 (2010) 1989–1992

Contents lists available at ScienceDirect

Surface & Coatings Technology

journal homepage: www.elsevier.com/locate/surfcoat

Thermal stability of AlCoCrCuFeNi high entropy alloy thin films studied by in-situ XRD analysis

V. Dolique [a,*], A.-L. Thomann [a], P. Brault [a], Y. Tessier [a], P. Gillon [b]

[a] Groupe de Recherche sur l'Energétique des Milieux Ionisés, UMR 6606 CNRS, Université d'Orléans BP 6744, 45067 Orléans Cedex 2, France
[b] ICARE CNRS 1C Av. de la Recherche Scientifique, 45071 Orléans Cedex 2, France

ARTICLE INFO

Available online 11 December 2009

Keywords:
Alloys
Thin films
Plasma sputtering deposition
Thermal stability

ABSTRACT

High entropy alloys (HEAs), containing five to thirteen metallic elements, with a concentration in the range of 5 to 35% for each element, exhibit very interesting properties (mechanical, tribological, formability, magnetism...). Their high mixing entropy promotes the formation of random solid solutions, amorphous alloys or nanocrystallized structures. Bulk pieces of these alloys are known to be stable at relatively high temperature (until 800 °C). We study the stability of AlCoCrCuFeNi thin film at temperatures in the range 110–810 °C. HEA thin films are deposited by magnetron sputtering from mosaic targets. In-situ X-ray diffraction (XRD) performed during annealing evidences damages of the film above 510 °C depending on the initial structure (or chemical composition) of the as-deposited HEA. Energy Dispersive Spectroscopy (EDS) and Scanning Electron Microscopy (SEM) analysis carried out before and after annealing show that partial evaporation of the thin film, crystalline phase transformation and chemical reaction with the substrate may take place during annealing.

1. Introduction

The large majority of the currently-used high-performance complex metallic alloys were developed in the 1970s. These alloys were typically composed of one or two principal elements, minor elements being added in order to modify their properties [1,2]. Since the 80s the study of new alloys containing more elements showed that an increase in the number of constitutive elements improves properties. If thirteen elements are arbitrarily selected, then, 7099 alloys are theoretically able to be synthesized, and even more, if some elements such as Si, C or B are added in low concentration. For example, AlCoCrCuFeNi, $AlCo_{0.5}CrCuFe_{1.5}Ni_{1.2}$ or $AlCo_{0.5}CrCuFe_{0.5}Ni_{0.12}B_{0.1}C_{0.15}$ [1] has been studied. An interesting property of such films is their hydrophobic character, which makes them alternative candidates for anti-adherent application and, for example, for replacement of Teflon [3]. To synthesize HEAs, different techniques are currently employed, such as rapid solidification, spray forming or mechanical alloying [1]. All these techniques lead to the formation of bulk or thick films of HEAs (>1 μm) [1,4–6]. In this study, HEA thin films have been synthesized by magnetron sputtering from mosaic targets. This technique allows deposition of HEA films in a wide range of chemical compositions. Stoichiometry can be easily controlled by varying the target powers and the relative surface fraction of each element on a given target. The thermal stability of AlCoCrCuFeNi thin films is studied by recording the X-ray diffraction spectra, in-situ, during the annealing process, which is performed in vacuum. Morphology and stoichiometry have been studied by Scanning Electron Microscopy (SEM) and Energy Dispersive Spectroscopy (EDS) before and after annealing. In a previous article [3] we have studied the relationship between microstructure, stoichiometry and surface morphology of this alloy. For the present study, we have chosen two samples, which exhibit two different structures: a mixture of BCC (110) and FCC (111) solid solutions for sample A, and a single FCC (111) structure for sample B.

2. Experimental procedure

To synthesize HEA thin films, DC magnetron sputtering technique is used with mosaic targets (patent no. WO/2008/028981). Three targets are placed in the chamber in order to ensure large overlapping of the sputtered atom fluxes of pure elements (99.99%). A detailed description of this system can be found in Refs. [3] and [7]. To adjust the stoichiometry of AlCoCrCuFeNi alloy, the relative surface fraction of each element on the target is calculated with TRIM software [8], taking into account the difference in sputtering yields. All experiments are performed at room temperature and 0.2 Pa argon pressure. The distance between target and substrate is 9 cm. A deposition time of 25 min is chosen to synthesize thin films of more than 1 μm thick on Si (100) substrates. To determine the morphology, grain size, film thickness and chemical composition, SEM (Carl Zeiss supra-40 FEG-SEM) is used with EDS (Brucker XFlash Detector 4010). X-ray diffraction (XRD) experiments are performed with a Brucker D8 diffractometer using the Cu Kα radiation and with a scanning speed of 40 °Cmin^{-1} [9]. The device,

* Corresponding author. Tel.: +33 2 38 49 45 18; fax: +33 2 38 41 71 54.
E-mail addresses: vincent.dolique@univ-orleans.fr (V. Dolique), anne-lise.thomann@univ-orleans.fr (A.-L. Thomann).

0257-8972/$ – see front matter © 2009 Elsevier B.V. All rights reserved.
doi:10.1016/j.surfcoat.2009.12.006

fitted out with a temperature chamber, gives the possibility to register XRD patterns between room temperature and 900 °C. The samples are kept under a residual pressure of $1.7 \cdot 10^{-2}$ Pa and the patterns are recorded during annealing in the 30°–50° 2θ range, with a 2θ-step of 0.031° and a step-time of 2 s (corresponding to a total acquisition time of 21 min per scanning at constant temperature).

3. Results

3.1. Characteristics of AlCoCrCuFeNi thin films before annealing

Fig. 1 shows SEM plane view of both samples before annealing. Differences in grain size and shape are observed. Spherical grains of 10–20 nm are found on sample B, and polyhedron grains of 100–200 nm on sample A. From XRD measurements (Fig. 2), two crystalline solid solution structures are evidenced: BCC (110) and FCC (111) for sample A, and FCC (111) for sample B. It has been evidenced in literature that very small variations in the chemical composition can induce lattice distortion, leading to the formation of one or another crystalline structure [3]. This fine dependence makes difficult to predict phase stability from the deposition parameters. The chemical composition of both samples obtained by EDS is given in Table 1. According to the deposition conditions (increased power on FeCoNi target), the relative atomic percentages of Fe, Co and Ni are higher in sample B than in sample A. However, the global compositions of both samples are very similar, since the variation of the percentage of one element never exceeds 9%. Despite this close chemical composition, the crystalline structures of both samples are different.

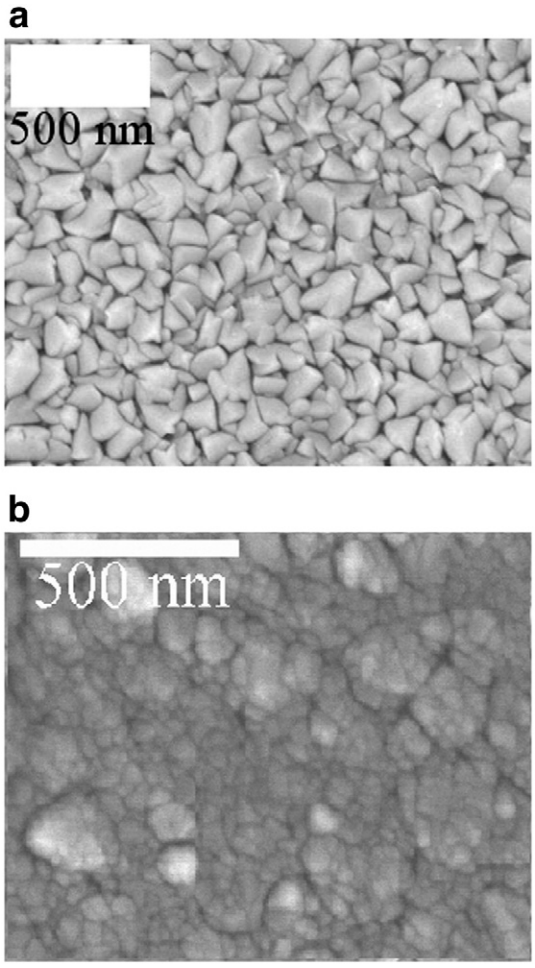

Fig. 1. SEM plane view micrographs of a) samples A and b) sample B.

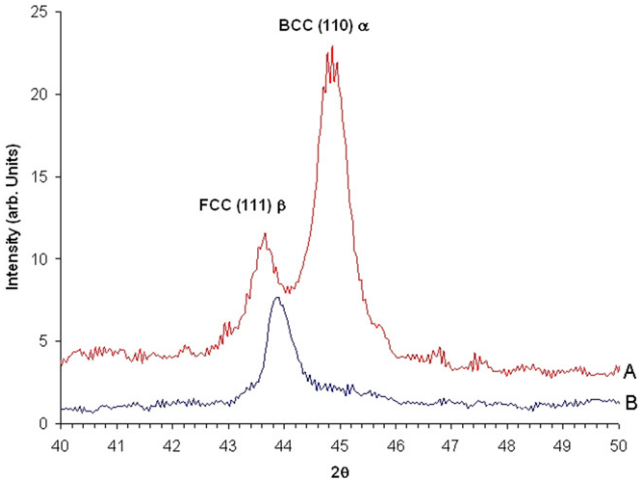

Fig. 2. XRD pattern of samples A and B before annealing.

A way to predict phase stability in these alloys could be to sum the concentrations of the elements which are expected to stabilize a FCC structure against a BCC one. We have recently shown [3] that the BCC structure was stabilized by the presence of Cr and Al in higher concentrations than the other elements. On the contrary, low Al contents associated with high Cu, Co and Ni ones are known to promote the formation of the FCC solid solution [10]. Indeed, it is known that the effect of Al concentration on the stabilization of one or the other structure is complex. At percentages lower than 15%, Al promotes the formation of FCC solid solution, whereas it stabilizes the BCC structure for percentages above. Since Al concentration is less than 15% in both samples, Al is considered as an FCC stabilized element. For sample A, the contribution of chemical elements leading to the formation of an FCC structure ([Cu] + [Co] + [Al] + [Ni] = 57%) is close to that of elements promoting the formation of a BCC structure ([Cr] + [Fe] = 43%). In the case of sample B, the concentration of FCC stabilizing elements is slightly higher (60%), which makes the structure to completely switch to FCC. Even if the Al concentration is below 15% in both samples, its higher percentage in sample A may help to drive the structure evolution towards a mixture of BCC and FCC structures.

3.2. Study of AlCoCrCuFeNi behaviour during annealing

During annealing, the recording time must be short enough so that the measurement is performed at a constant temperature. We have chosen to plot the XRD patterns in the range between $2\theta = 30°$ and $2\theta = 50°$ because peaks of the BCC and FCC solid solution are present. No evolution of the crystalline structure is observed on sample B until 510 °C (Fig. 3). Above this temperature, the FCC (111) peak of the HEA disappears, and new peaks are visible on the spectra. The one at $2\theta = 45.4°$, whose intensity increases between 710 °C and 810 °C, can be attributed to Cu_3Si (312) [11] or NiSi (211) [12] or SiO_2 (111) reflections. Surprisingly no other peaks expected for these compounds are detected. This prevents unambiguous determination of the corresponding compound. However, the peak at $2\theta = 44.9°$, which appears at 710 °C and disappears at 810 °C, may also be attributed to Cu_3Si alloy. Moreover, SEM analysis observations evidence the presence of holes and kinds of inclusions (Fig. 4), which are characteristics of silicide formation [13]. The presence of these peaks attributed to a Si compound indicates first, that the substrate has been modified during the annealing process (the Si (200) is not detected anymore) and second that the HEA film has been partly evaporated. The phenomenon of preferential evaporation in sample B is checked by EDS analysis performed after annealing (Table 1): Cu and Ni are the only remaining elements. The high Ni concentration found by EDS is in agreement with the shift at 710 °C of the FCC (111) HEA peak towards a higher angle ($2\theta = 44.4°$), which is the value corresponding to pure Ni.

Table 1
Conditions of deposition and chemical composition.

Sample	Conditions of deposition						
	Pressure (Pa)	Power (W) target 1 (CuCr)	Power (W) target 2 (FeCoNi)	Power (W) target (Al)	Time of deposition (s)	Temperature (°C)	
A	0.25	190	170	20	1500	30	
B	0.25	180	310	15	1500	30	
	Chemical composition						
	Elements	Al	Co	Cr	Cu	Fe	Ni
	Structure	FCC	HCP	BCC	FCC	BCC	FCC
Before annealing							
A	Global	13	14	27	11	16	19
B	Global	10	17	18	9	22	24
After annealing							
A	Area 1	37	0	57	0	2	2
	Area 2	34	14	7	14	17	14
	Global	34	7	31	12	8	8
B	Global	0	0	0	17	0	83

The study of sample B annealing has shown that the integrity of the HEA thin film is kept until 510 °C. Above this temperature, preferential evaporation takes place leading to the formation of a pure Ni phase, which is the main remaining element. The small amount of copper still present in the film has chemically reacted with the substrate to form Cu_3Si.

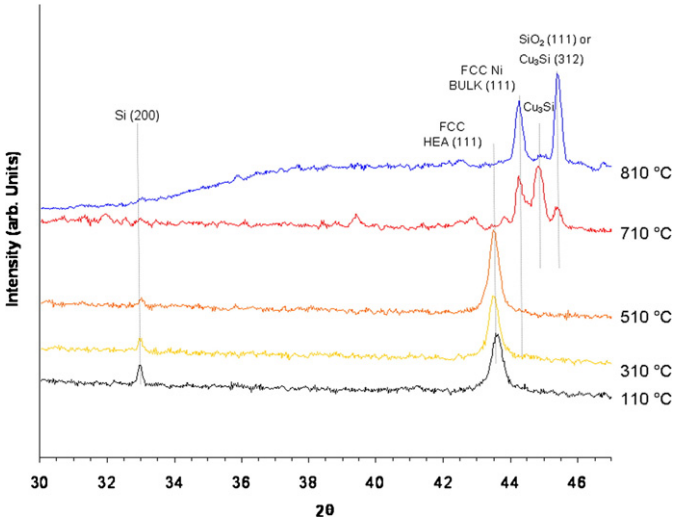

Fig. 3. Evolution of XRD patterns during annealing of sample B.

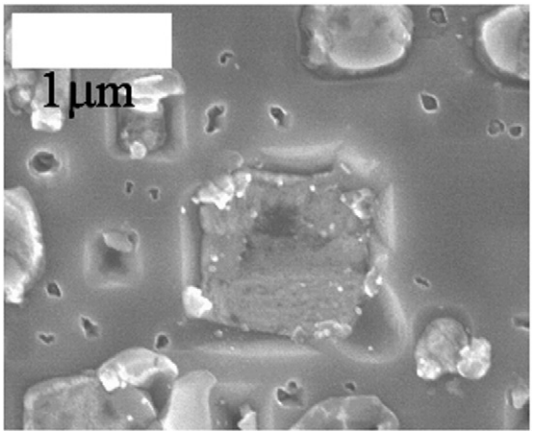

Fig. 4. SEM micrographs after annealing of sample B.

The same kind of annealing has been performed on sample A (Fig. 5). At room temperature, sample A exhibits a mixture of BCC (110) and FCC (111) solid solutions. At 130 °C and 310 °C, a small shift of FCC (111) and BCC (110) peaks toward small angles and a change of the relative intensities of the peaks are observed. These trends indicate that re-organisation, certainly due to atomic diffusion, takes place in the HEA structure even at this relatively low temperature. Above 310 °C, a more complex transition takes place, which leads to the disappearance of the BCC structure and to the appearance of reflections at angles $2\theta = 40.4°$, 42.5°, 47.3° and 49.8°; the FCC phase of AlCoCrCuFeNi ($2\theta = 42.8°$) remains present. The detected peaks can be attributed to several binary alloys, for example $AlCr_2$, Al_8Cr_5 (JCPDS numbers: 29-0016 and 47-1466), AlCu or FeCr. We have not found a single alloy consistent with all peaks. SEM images (Fig. 6) show two different areas of various contrasts. Differences in composition are clearly evidenced from global and local EDS analyses (Table 1). In area 1, there is neither Co nor Cu, but high concentrations of Al and Cr. This is thus compatible with the assumption of the formation of the binary alloys $AlCr_2$ or Al_8Cr_5. EDS analysis of area 2 evidences that all chemical elements remain present but in different proportions than in the as-deposited thin film. The Al concentration is higher (34% instead of 13%) and Cr one lower (7% instead of 27%). The presence of these areas of different chemical compositions is also an indication that atomic diffusion takes place on this sample when the temperature increases. Small black grains are visible in Fig. 6 especially in area 2. EDS analysis performed on the grains and in-between gives the same

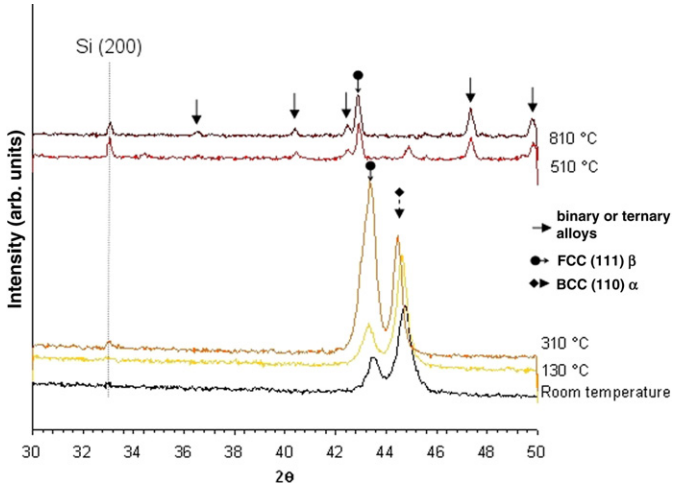

Fig. 5. Evolution of XRD patterns during annealing of sample A.

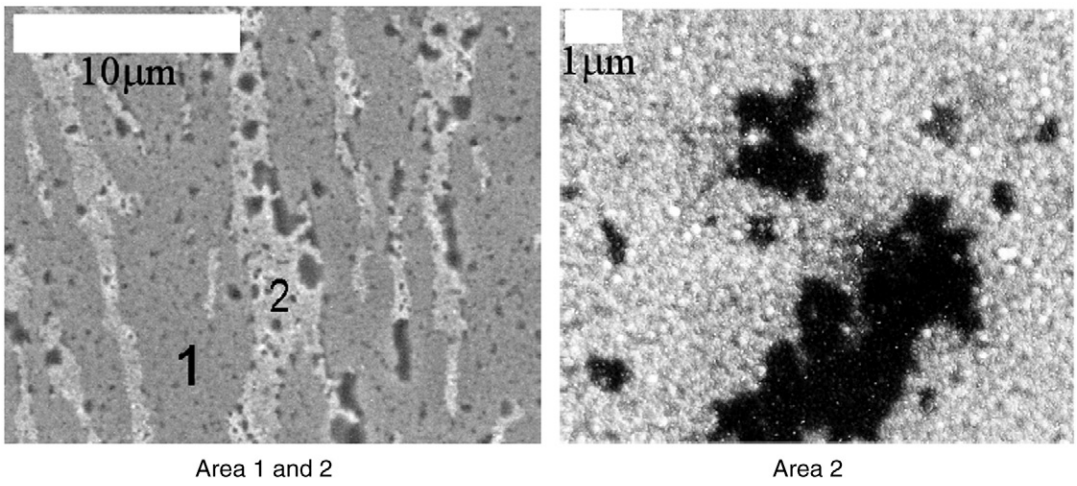

Fig. 6. SEM micrographs after annealing of sample A.

composition. We think that they are due to carbon contamination occurring during annealing.

Thus, even if modification of the initial HEA structure is observed at lower temperatures for sample A (310 °C), the thin film encounters less drastic changes at higher temperatures. All the chemical elements are still present but in various inter-metallic phases. More generally, we have shown that the initial structure (which depends on the stoichiometry) influences the thermal stability of the thin films. Sample A and sample B do not exhibit the same structure and lead to different behaviours during annealing, especially above 510 °C. Above this temperature, the integrity of sample B HEA film is severely affected (evaporation and formation of silicides), whereas a metallic thin film is always present in sample A, even if intermetallics have been formed. The reason for such different behaviours is not yet well understood. It is interesting to compare this work with what is reported in literature. For bulk HEAs, C.J. Tong et al. [6,14] have shown that HEAs exhibited superior high temperature mechanical behaviour until 800 °C. Above this temperature, mechanical properties are deteriorated, which indicates that the alloys are damaged. Y.Y. Chen et al. [5] have studied the Differential Scanning Calorimetry thermograms of AlCoCrCuFeNiSi HEA, spanning from room temperature to 1400 °C: weak endothermic reaction at 1010 °C has been evidenced, which is attributed to a phase transition. The works cited above show that bulk HEAs are stable until temperature higher than films studied here. However, L.H. Wen [15] has studied the thermal behaviour of bulk AlCoCrCuFeNi alloy by XRD between 500 °C and 1000 °C. He has found that the only change during annealing is the relative intensity of the FCC and BCC peaks. Our results on sample A are very similar, since the FCC becomes the main phase at 310 °C. Unfortunately, authors do not give all the annealing conditions, thus it is difficult to make further comparisons. Indeed, with the annealing being performed under vacuum in our case, evaporation is expected to be promoted compared to annealing under controlled atmosphere. It is interesting to note that in the case of sample B, the observed degradation is partly due to reactivity between chemical elements present in the HEA and the silicium used as substrate. In this case, we did not manage to test the thermal stability of the HEA, but the one of the HEA/Si interface. The behaviour during annealing would certainly be different with another substrate. However, an important result is that the HEA thin films studied in the present work are stable until a temperature just below the bulk HEA degradation temperature.

4. Conclusion

Two HEA thin films with stoichiometries close to equimolarity have been synthesized by magnetron sputtering from mosaic targets. It has been shown that a small difference of the global stoichiometry leads to a different structure, thermal stability and evolution during annealing. Both samples are found stable (no drastic phase modification) until 510 °C, but exhibit different behaviours at higher temperature. For sample B, above 510 °C, the FCC (111) peak of the HEA disappears and EDS analysis evidences a phenomenon of preferential evaporation. The remaining chemical elements are included in a pure Ni phase and a Cu silicide compound. For sample A, above 310 °C, a phase transition takes place, which leads to the disappearance of the BCC structure and to the formation of AlCr binary alloy phases. Chemical analysis of sample A surface showed segregation of elements. Thermal stability of HEA thin films found in this work is compatible with replacement of Teflon® in low working temperature applications such as food industry or cosmetic packaging.

Acknowledgements

The CME (Centre de Microscopie Electronique) of the University of Orleans and V. Pelosin of the LMPM laboratory (University of Poitiers) are gratefully acknowledged for SEM, EDS and XRD analysis. This work was financially supported by the CNRS. Referees are gratefully acknowledged for great help.

References

[1] J.-W. Yeh, Ann. Chim. Sci. Mater. 31 (6) (2006) 663.
[2] J.-W. Yeh, S.-K. Chen, J.-Y. Gan, T.-S. Chin, T.-T. Shun, C.H. Tsau, S.-Y. Chang, Adv. Eng. Mater. 6 (2004) 299.
[3] V. Dolique, A.-L. Thomann, P. Brault, Y. Tessier, P. Gillon, Mater. Chem. Phys. 117 (2009) 142.
[4] Y.-J. Zhou, Y. Zhang, Y.-L. Wang, G.-L. Chen, Mater. Sci. Eng. A 454–455 (2007) 260.
[5] Y.-Y. Chen, T. Duval, U.-D. Hung, J.-W. Yeh, H.-C. Shih, Corros. Sci. 47 (2005) 2257.
[6] C.-J. Tong, M.R. Chen, S.K. Chen, J.W. Yeh, T.-T. Shun, S.J. Lin, S.Y. Chang, Metall. Mater. Trans. A 36 A (2005) 1263.
[7] P. Plantin, A.-L. Thomann, P. Brault, B. Dumax, J. Mathias, T. Sauvage, A. Pineau, Surf. Coat. Technol. 200 (2005) 408.
[8] M. Mayer 1997 SIMNRA user's guide, IPP 9/113 (Garching: Max-Planck-Institut fur Plasma Physik) SIMNRA homepage http://www.rzg.mpg.de/mam.
[9] V. Dolique, M. Jaouen, T. Cabioc'h, F. Pailloux, Ph. Guérin, V. Pélosin, J. Appl. Phys. 103 (2008) 083527.
[10] C.-C. Tong, J.-W. Yeh, T.-T. Shun, S.-K. Chen, Y.-S. Huang, H.-C. Chen, Mater. Lett. 61 (2007) 1.
[11] S.-T. Lin, Y.-L. Kuo, C. Lee, Appl. Surf. Sci. 220 (2003) 349.
[12] M. Bhaskaran, S. Sriram, T.S. Perova, V. Ermakov, G.J. Thorogood, K.T. Short, A.S. Holland, Micron 40 (2009) 89.
[13] B.-S. Suh, Y.-J. Lee, J.-S. Hwang, C.-O. Park, Thin Solid Films 348 (1999) 299.
[14] C.-J. Tong, M.-R. Chen, S.-K. Chen, J.-W. Yeh, T.-T. Shun, S.-J. Lin, S.-Y. Chang, Metall. Mater. Trans. A 36A (2005) 881.
[15] L.-H. Wen, H.-C. Kou, J.-S. Li, H. Chang, X.-Y. Xue, L. Zhou, Intermetallics 17 (2009) 266.